State-Variable Steady-State Analysis of a Controlled Current Induction Motor Drive

THOMAS A. LIPO, SENIOR MEMBER, IEEE, AND EDWARD P. CORNELL, MEMBER, IEEE

Abstract—**The exact equations defining steady-state operation of a controlled current induction motor drive system are derived by solving the system state equations in the stationary reference frame. These equations, which assume ideal current filtering, eliminate the difficulties involved in taking derivatives of discontinuous currents by defining a pair of pseudocurrent variables. Effects of saturation are included by using the slope ratio method. Electromagnetic torque and current pulsations are computed for various load conditions, and experimental confirmation of the calculated results is made. Similarities and differences to voltage controlled characteristics are presented. It is shown that normal open-loop operation occurs on the unstable side of the torque-slip characteristic necessitating the use of feedback control for stable operation.**

INTRODUCTION

MOST INVERTERS in present use can be designated controllable-voltage adjustable-frequency sources, since the output terminal voltage is essentially independent of current. Recently, however, the useful features of inverters in which the current rather than voltage appears essentially as the independent variable have been recognized. Since a large portion of electrical equipment which utilizes ac power over a range of frequencies requires current of approximately constant amplitude, this type of inverter appears to have inherent advantages. Typical applications include ac motor drives which are controlled to develop constant motor torque over a fixed speed range. In addition, the simplicity of the inverter design, low cost, and regeneration capability make the controlled current source inverter (CCI) an attractive alternative to conventional controllable-voltage source inverters.

Although the principle of a controlled current source has been recognized for decades [1] and is, in fact, the principle behind operation of present-day HVDC links [2], the application to ac motor drives is of a much more recent nature [3]–[11]. Thus far, however, analyses of motor performance have been conducted by considering only the fundamental components of the ac line current [7], [8]. Although such an approach yields valuable information regarding quasi-stationary behavior, a more detailed solution is required if such important effects as motor heating and torque pulsations are to be accurately evaluated.

Paper TOD-75-45, approved by the Static Power Converter Committee of the IEEE Industry Applications Society for presentation at the IEEE 1974 Industry Applications Society Annual Meeting, Pittsburgh, Pa., October 7–10. Manuscript released for publication May 5, 1975.

The authors are with the General Electric Company, Schenectady, N. Y. 12301.

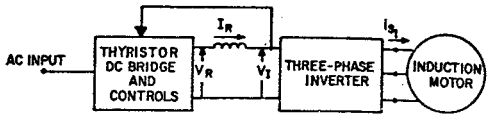

Fig. 1. Basic controlled current induction motor (CCI) drive system.

Probably the most popular approaches for analysis of ac motor drives which employ nonsinusoidal sources are harmonic superposition techniques using either symmetrical components [12] or multiple reference frames [13]. Although such methods are applicable to a CCI motor drive, the current in the lines of the motor are essentially "square wave" in nature. Numerous harmonics must be employed for accurate approximation of the input current waveshape.

This paper presents a simple alternative procedure for the steady-state analysis of an induction motor operating from a controlled current source. The method, which uses state variable techniques [14], [15], results in an exact closed form solution avoiding entirely the troublesome "Gibbs phenomena" or ringing in the solution which is characteristic of approaches using harmonic superposition. Since the solution is explicitly known, the effect of all parameters on motor performance can be rapidly and conveniently evaluated.

DESCRIPTION OF SYSTEM

A simplified diagram of the system considered in this paper is given in Fig. 1. Basically, the system consists of a controlled rectifier bridge, a dc link filter choke, a three-phase inverter, and an induction motor. The controlled rectifier bridge and choke together form a dc current source which supplies constant regulated dc current to the inverter. The inverter shown in Fig. 2 is the autosequential commutated inverter described by Ward [4] and appears to be the type in widest use. Although a number of alternative schemes are possible [3], [5], [8], they differ primarily in the means by which commutation is accomplished. Hence, the input–output terminal characteristics remain essentially the same. In Fig. 2, thyristors $T1$–$T6$ switch the load current at a rate established by the inverter control and establish the inverter output frequency. Capacitors $C1$–$C6$ provide the necessary com-

mutation energy while diodes $D1$–$D6$ isolate the capacitors from the load. A diagram illustrating the thyristor gating sequence and resulting line currents is shown in Fig. 3.

In this paper the following is assumed.

a) The thyristor bridge and dc choke may be considered as an ideal adjustable current source having infinite impedance. Hence, the dc link current I_R is assumed constant.

b) The inverter is considered as a zero impedance instantaneous switching device. That is, the effects of the commutating circuit will be neglected. Although assumptions a) and b) essentially eliminate the effect of source parameters on motor behavior, these assumptions have been found to be reasonably valid over low and medium frequency operating ranges.

c) The induction machine is considered an ideal machine in which the stator and rotor windings are distributed so as to always produce a single sinusoidal space distribution of MMF in the air gap.

d) The system is in the steady-state. In particular, the rotor speed is assumed to be constant. Although harmonic torques resulting from supply harmonics tend to produce speed oscillations, it is assumed that the rotor inertia is sufficiently large so as to minimize this effect.

e) All parameters of the machine are assumed to be constant.

f) The motor is assumed to be a wye-connected three-wire system. If the motor is delta-connected, it can be shown that if c) is valid, then this machine can be replaced by an equivalent wye-connection without altering its characteristics.

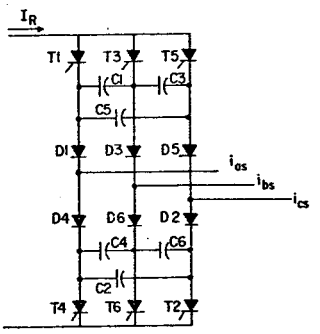

Fig. 2. Current-source inverter with autosequential commutation.

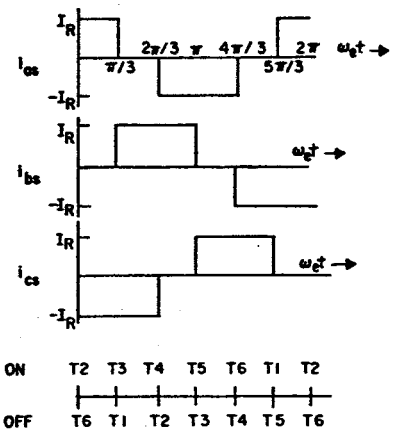

Fig. 3. Inverter gating sequence and resulting line currents.

SYSTEM EQUATIONS

The differential equations which describe transient behavior of an induction machine are conveniently expressed by transforming the stator and rotor phase variables to dq axes fixed either on the stator or rotor or rotating at synchronous speed. When the reference frame is fixed in the stator, the resulting equations are generally termed Stanley's Equations [16]. Using the notation of Krause and Thomas [17], these equations, expressed in per unit, are given in matrix form by

$$\begin{bmatrix} v_{qs}^{s} \\ v_{ds}^{s} \\ 0 \\ 0 \end{bmatrix} = \begin{bmatrix} r_s + \frac{p}{\omega_b} x_s & 0 & \frac{p}{\omega_b} x_m & 0 \\ 0 & r_s + \frac{p}{\omega_b} x_s & 0 & \frac{p}{\omega_b} x_m \\ \frac{p}{\omega_b} x_m & -\frac{\omega_r}{\omega_b} x_m & r_r' + \frac{p}{\omega_b} x_r' & -\frac{\omega_r}{\omega_b} x_r' \\ \frac{\omega_r}{\omega_b} x_m & \frac{p}{\omega_b} x_m & \frac{\omega_r}{\omega_b} x_r' & r_r' + \frac{p}{\omega_b} x_r' \end{bmatrix} \times \begin{bmatrix} i_{qs}^{s} \\ i_{ds}^{s} \\ i_{qr}'^{s} \\ i_{dr}'^{s} \end{bmatrix}. \quad (1)$$

In these equations, the superscript s is employed to denote that the $d-q$ axes have been fixed in the stator. A p denotes the operator d/dt. Although six equations are generally required to completely define the machine response, the two zero-sequence equations have been omitted since the sums of the stator as well as rotor currents are zero. Also in (1), ω_b is the base electrical angular velocity used to obtain the per unit machine parameters, ω_r is the equivalent electrical angular velocity of the rotor, and r_s and r_r' are stator and referred rotor resistance. The quantities x_s, x_m, and x_r' are the stator self-, mutual, and rotor self-reactance referred to the stator, respectively.

The voltages v_{ds}^s and v_{qs}^s are an equivalent set of voltages related to the phase voltages by the equations

$$v_{qs}^s = v_{as} \tag{2}$$

$$v_{ds}^s = \frac{1}{\sqrt{3}}(v_{cs} - v_{bs}). \tag{3}$$

The $d - q$ stator currents are similarly related to the stator phase currents by

$$i_{qs}^s = i_{as} \tag{4}$$

$$i_{ds}^s = \frac{1}{\sqrt{3}}(i_{cs} - i_{bs}). \tag{5}$$

The stator-referred $d - q$ rotor currents are expressed in terms of the rotor phase currents by

$$i_{qr}'^s = \frac{N_r}{N_s}\left[i_{ar}\cos\theta_r + \frac{1}{\sqrt{3}}(i_{cr} - i_{br})\sin\theta_r\right]. \tag{6}$$

$$i_{dr}'^s = \frac{N_r}{N_s}\left[-i_{ar}\sin\theta_r + \frac{1}{\sqrt{3}}(i_{cr} - i_{br})\cos\theta_r\right]. \tag{7}$$

In order to obtain (2)–(7), it is again necessary to assume that the sum of the stator currents and the sum of the rotor currents are zero. In (6) and (7), N_r/N_s is the effective rotor-to-stator turns ratio. θ_r denotes the relative displacement in electrical radians of the ar rotor axis with respect to the as axis, which have been assumed aligned at $t = 0$. That is, when speed is assumed constant, $\theta_r = \omega_r t$.

In addition to the motor current it is generally desirable to solve for the electromagnetic torque developed by the machine. When peak rated line-to-neutral voltage and peak rated line current are chosen as base quantities, the electromagnetic torque expressed in terms of the $ds - qs$ variables is

$$T_e = x_m(i_{qs}^s i_{dr}'^s - i_{ds}^s i_{qr}'^s). \tag{8}$$

Although (1)–(7) serve to completely define machine behavior regardless of the terminal conditions, it can be noted that voltages rather than currents appear as independent variables. When stator currents are known explicitly, it is apparent that only the third and fourth equation corresponding to the third and fourth row of (1) are independent in the solution. The first and second equations constitute two auxiliary relations which serve to define motor terminal voltage but which are not otherwise required in the solution. Since the stator currents can be considered as inputs to the rotor voltage equations, these terms can be transferred to the left side and the two rotor equations written as

$$\frac{\omega_r}{\omega_b}x_m i_{ds}^s - \frac{p}{\omega_b}x_m i_{qs}^s = \frac{p}{\omega_b}x_r' i_{qr}'^s + r_r' i_{qr}'^s - \frac{\omega_r}{\omega_b}x_r' i_{dr}'^s \tag{9}$$

$$-\frac{\omega_r}{\omega_b}x_m i_{qs}^s - \frac{p}{\omega_b}x_m i_{ds}^s = \frac{p}{\omega_b}x_r' i_{dr}'^s + r_r' i_{dr}'^s + \frac{\omega_r}{\omega_b}x_r' i_{qr}'^s. \tag{10}$$

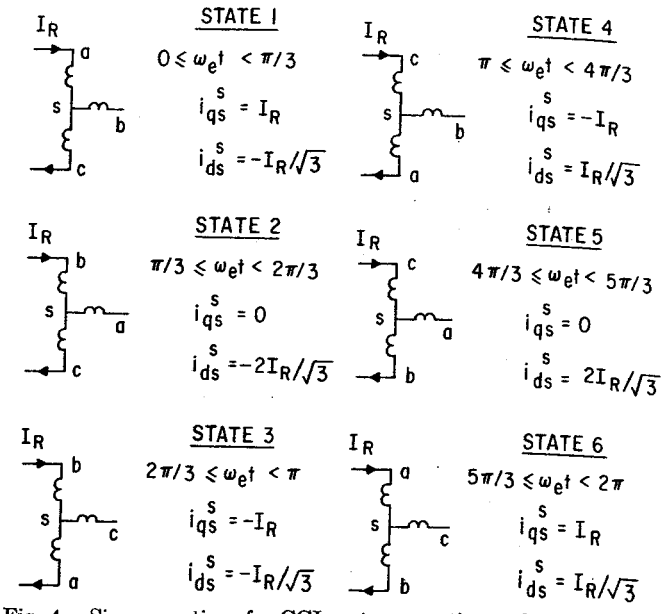

Fig. 4. Six connections for CCI motor operation and resulting $d-q$ stator currents.

In order to complete the problem definition the $d - q$ stator current inputs to the two system equations, (9) and (10), must be specified. In Fig. 4 the circuit connections corresponding to the six inverter states are summarized. The equations which define the $d - q$ stator currents for each of the six states follow directly from (4) and (5) and are given next to the appropriate sketch.

Equations (9) and (10) together with the equations which specify the input currents completely define system behavior when the dc link current is assumed constant and the inverter is symmetrically switched in accordance with Fig. 3. Moreover, these equations are equally valid for constant speed transients as well as steady-state. It can be observed from Fig. 4 that the input currents i_{qs}^s and i_{ds}^s are only piecewise continuous over a cycle. Although the first input term presents no problem, it is apparent that the second term contributes impulse functions at the switching instants $\omega_e t = 0$, $\pi/3$, $2\pi/3$, etc. In order to avoid the difficulties encountered with impulse functions the derivative term can be removed by an appropriate change in variables.

It is useful to consider new pseudocurrent variables defined as

$$i_Q = i_{qr}'^s + \frac{x_m}{x_r'}i_{qs}^s \tag{11}$$

$$i_D = i_{dr}'^s + \frac{x_m}{x_r'}i_{ds}^s. \tag{12}$$

It should be noted that this change of variable is equivalent to specifying rotor flux linkages rather than currents as state variables. Equations (11) and (12) imply that

$$i_{qr}'^s = i_Q - \frac{x_m}{x_r'}i_{qs}^s \tag{13}$$

$$i_{dr}'^s = i_D - \frac{x_m}{x_r'}i_{ds}^s \tag{14}$$

$$\frac{p}{\omega_b} i_{qr}'^s = \frac{p}{\omega_b} i_Q - \frac{x_m}{x_r'} \frac{p}{\omega_b} i_{qs}^s \tag{15}$$

$$\frac{p}{\omega_b} i_{dr}'^s = \frac{p}{\omega_b} i_D - \frac{x_m}{x_r'} \frac{p}{\omega_b} i_{ds}^s. \tag{16}$$

Substituting (13)–(16) into (9) and (10) yields the following equations in terms of the modified rotor current variables:

$$\frac{r_r' x_m}{x_r'} i_{qs}^s = \frac{p}{\omega_b} x_r' i_Q + r_r' i_Q - \frac{\omega_r}{\omega_b} x_r' i_D \tag{17}$$

$$\frac{r_r' x_m}{x_r'} i_{ds}^s = \frac{p}{\omega_b} x_r' i_D + r_r' i_D + \frac{\omega_r}{\omega_b} x_r' i_Q. \tag{18}$$

It can be noted that the derivative terms have now been eliminated. Since the input does not now contain impulse functions it is evident that the modified current variables are clearly continuous functions even at the instants at which the stator currents are discontinuous. Hence, these equations are amenable to conventional state-variable techniques.

When (17) and (18) are solved for the derivative terms, they can be written in matrix form as

$$\frac{p}{\omega_b}\begin{bmatrix} i_Q \\ i_D \end{bmatrix} = \begin{bmatrix} \dfrac{-r_r'}{x_r'} & \dfrac{\omega_r}{\omega_b} \\ \dfrac{-\omega_r}{\omega_b} & \dfrac{-r_r'}{x_r'} \end{bmatrix} \begin{bmatrix} i_Q \\ i_D \end{bmatrix} + \frac{r_r' x_m}{(x_r')^2} \begin{bmatrix} i_{qs}^s \\ i_{ds}^s \end{bmatrix}. \tag{19}$$

Equation (19) can be written in conventional state-variable notation as

$$\frac{p}{\omega_b} \bar{i}_{QD} = \tilde{A} \bar{i}_{QD} + b \bar{i}_{qds}^s \tag{20}$$

where

$$\bar{i}_{QD} = [i_Q, i_D]^t \tag{21}$$

$$\bar{i}_{qds}^s = [i_{qs}^s, i_{ds}^s]^t \tag{22}$$

and t denotes the transpose. Definitions of the quantities $\tilde{A}$ and b are clearly implied by the context.

SYMMETRY RELATIONS

In general, because the $d - q$ axes input currents change six times per cycle, a closed form solution of (19) over a complete cycle is difficult. However, because of the symmetric nature of the inverter switching it can be shown that it is not generally necessary to obtain the solution over an entire cycle [15].

By reference to Fig. 3, it is clear that the three stator currents are half-wave symmetric. That is, for any two time instants relatively displaced by 180 electrical degrees

$$i_{as}(\omega_e t) = -i_{as}(\omega_e t + \pi) \tag{23}$$

$$i_{bs}(\omega_e t) = -i_{bs}(\omega_e t + \pi) \tag{24}$$

$$i_{cs}(\omega_e t) = -i_{cs}(\omega_e t + \pi). \tag{25}$$

Also, because of phase symmetry, the three currents are mutually displaced by 120 electrical degrees, or

$$i_{as}(\omega_e t + \pi/3) = i_{cs}(\omega_e t + \pi) \tag{26}$$

$$i_{bs}(\omega_e t + \pi/3) = i_{as}(\omega_e t + \pi) \tag{27}$$

$$i_{cs}(\omega_e t + \pi/3) = i_{bs}(\omega_e t + \pi). \tag{28}$$

Substracting (26)–(28) from (23)–(25), respectively, yields

$$i_{as}(\omega_e t + \pi/3) = -i_{bs}(\omega_e t) \tag{29}$$

$$i_{bs}(\omega_e t + \pi/3) = -i_{cs}(\omega_e t) \tag{30}$$

$$i_{cs}(\omega_e t + \pi/3) = -i_{as}(\omega_e t). \tag{31}$$

Equations (29)–(31) imply that if the current is specified at any time instant, then the currents 60 electrical degrees later are specified as well. Substituting (29)–(31) into (4) and (5) yields an equivalent relation in terms of the corresponding $d - q$ axes currents.

$$i_{qs}^s(\omega_e t + \pi/3) = \frac{1}{2} i_{qs}^s(\omega_e t) + \frac{\sqrt{3}}{2} i_{ds}^s(\omega_e t) \tag{32}$$

$$i_{ds}^s(\omega_e t + \pi/3) = \frac{-\sqrt{3}}{2} i_{qs}^s(\omega_e t) + \frac{1}{2} i_{ds}^s(\omega_e t). \tag{33}$$

Hence, a similar type of symmetry exists for the $d - q$ stator currents. Moreover, because i_{qs}^s and i_{ds}^s act as inputs to a set of linear equations it is apparent that in the steady-state, an equivalent set of relations apply for the $d - q$ pseudocurrents. That is, in matrix form

$$\bar{i}_{QD}(\omega_e t + \pi/3) = \tilde{S} \bar{i}_{QD}(\omega_e t) \tag{34}$$

where

$$\tilde{S} = \begin{bmatrix} \dfrac{1}{2} & \dfrac{\sqrt{3}}{2} \\ \dfrac{-\sqrt{3}}{2} & \dfrac{1}{2} \end{bmatrix}. \tag{35}$$

Equation (34) has considerable significance since it implies that if the solution is known over any 60° interval such as $0 \leq \omega_e t < \pi/3$, then the solution is completely defined over the interval $\pi/3 \leq \omega_e t < 2\pi/3$. Furthermore, the solution is also known over the remaining portion of an entire cycle by using this equation repetitively.

STATE-VARIABLE ANALYSIS

Since the input variables are constant over the interval $0 \leq \omega_e t < \pi/3$, the formal solution of (20) is

$$\bar{i}_{QD}(\omega_e t) = \exp(\tilde{A}\omega_b t) \bar{i}_{QD}(0) + \omega_b \int_0^t \exp[\tilde{A}\omega_b(t - \tau)] b \bar{i}_1 \, d\tau \tag{36}$$

where from Fig. 4 during state 1,

$$\bar{i}_{qds^s} = \bar{i}_1 = \begin{bmatrix} I_R \\ -I_R/\sqrt{3} \end{bmatrix}. \quad (37)$$

In particular, from Fig. 3 at the time instant $t = \pi/3\omega_e = T$, since T, b, and $\bar{i}_1$ are constants,

$$\bar{i}_{QD}(\pi/3) = \exp(\bar{A}\omega_b T)\bar{i}_{QD}(0) + \exp(\bar{A}\omega_b T)\left[\int_0^T \exp(-\bar{A}\omega_b \tau)\, d(\omega_b \tau)\right] b\bar{i}_1. \quad (38)$$

Upon completing the integration, the pseudocurrents at the time instant $\omega_e t = \pi/3$ can be solved in terms of the initial currents at $t = 0$ and the input currents. Noting $T = \pi/3\omega_e$ and defining

$$f_R = \omega_e/\omega_b. \quad (39)$$

Equation (38) can be written

$$\bar{i}_{QD}(\pi/3) = \exp(\bar{A}\pi/3f_R)\bar{i}_{QD}(0) + [\exp(\bar{A}\pi/3f_R) - \bar{I}]\bar{A}^{-1}b\bar{i}_1 \quad (40)$$

where $\bar{I}$ is the identity matrix.

In general, the $d - q$ rotor currents are unknown at both time instants $\omega_e t = 0$ and $\pi/3$. However, because of symmetry the solution at these two time instants must be related by (34). That is

$$\bar{i}_{QD}(\pi/3) = \bar{S}\bar{i}_{QD}(0). \quad (41)$$

Solving (40) and (41), the initial condition $\bar{i}_{QD}(0)$ as a unique function of motor parameters and system inputs is

$$\bar{i}_{QD}(0) = [\bar{S} - \exp(\bar{A}\pi/3f_R)]^{-1} \cdot [\exp(\bar{A}\pi/3f_R) - \bar{I}]\bar{A}^{-1}b\bar{i}_1. \quad (42)$$

Having obtained the initial condition for the time interval the solution is known throughout the entire interval by (6). In particular

$$\bar{i}_{QD}(\omega_e t) = \exp(\bar{A}\omega_e t)\bar{i}_{QD}(0) + [\exp(\bar{A}\omega_e t) - \bar{I}]\bar{A}^{-1}b\bar{i}_1 \quad (43)$$

where $0 \leq \omega_e t < \pi/3$. The solution for the remaining five intervals is immediately known by virtue of symmetry, (34).

It should be noted that although the solution has been completely defined in terms of basic motor parameters, speed, and input current, the solution is only implicitly known by means of the defined quantities $\bar{A}$ and b. In some cases it would be desirable to obtain a solution wherein these variables appear explicitly. This can in fact be done by substituting explicitly for $\bar{A}$ and b in (42) and (43). Unfortunately, the resulting equations become quite cumbersome in spite of the fact that the system is second order and do not appear to lend any additional insight into the problem. Hence, the explicit form for these equations has not been included in this paper.

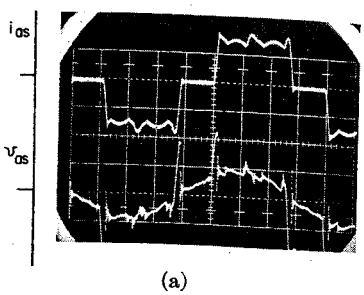

(a)

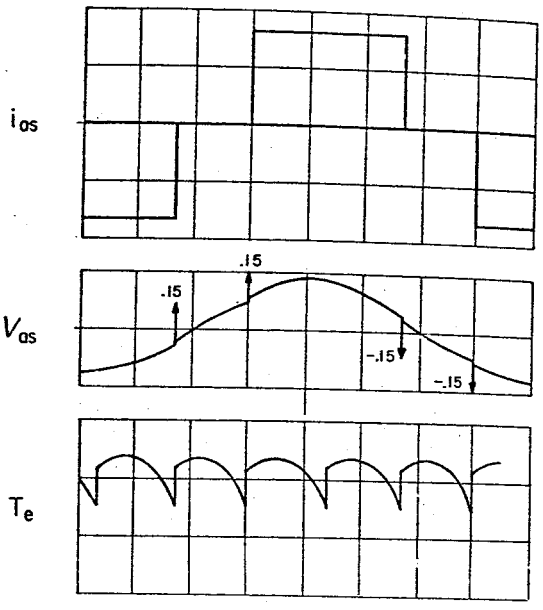

(b)

Fig. 5. (a) Experimental. (b) Calculated. Comparison of computed and measured results. $I_R = 82$ A; $\omega_e = 188.5$ rad/s; slip = 0.04; $T_L = 102$ N·m SCALE: $I_{as} - 50$ A/div; $V_{as} - 100$ V/div; $T_e - 50$ N·m/div Time Axis $-$ 4.17 ms (45°)/div.

In addition to the stator and rotor currents, the stator voltages are of considerable interest. The solution for the stator terminal voltages as well as for electromagnetic torque is given in Appendix I.

COMPARISON OF COMPUTED AND TESTED RESULTS

In order to verify the analysis, the equations which have been developed were evaluated using a digital computer, and the computed solution was compared to tested results. The induction machine used for purposes of comparison was a 230 V, 4 pole, 25 hp induction machine. A summary of the relevant parameters is given in Appendix II.

Fig. 5 shows a comparison of the computed results with measurements from the actual system. Although not measurable in the physical system, the instantaneous electromagnetic torque obtained from the computer solution is also plotted. For the case shown, the inverter frequency was set at one-half rated frequency (30 Hz) and the dc link current was adjusted until the fundamental component of motor line current was at rated value. The slip of the motor was fixed at 0.02. Although the computer program was written to compute per unit

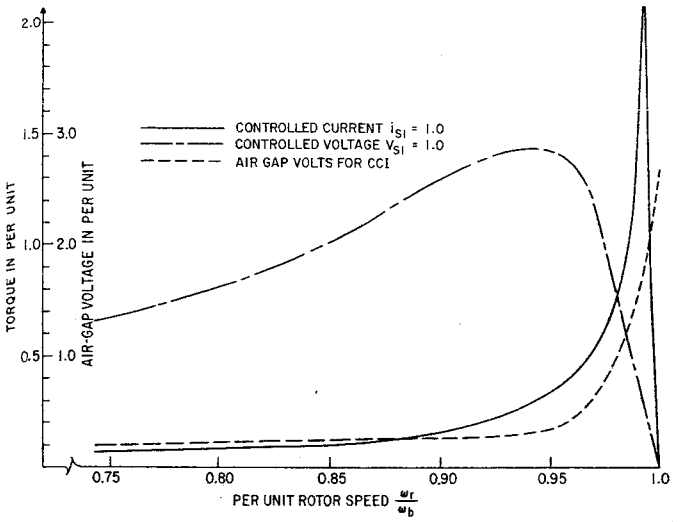

Fig. 6. Steady-state torque-speed characteristics for controlled current and controlled voltage operation.

quantities, all variables have been converted to normal units for purposes of comparison.

The location of the impulses computed from the digital computer solution is indicated with an arrow. The strength of the "area" of the impulse is adjacent to the arrow. It can be noted that the amplitudes of the voltages and locations of the pulses in the voltage waveshapes are in good agreement. In the actual system, of course, the voltage pulses are finite amplitude being limited by the commutating capability of the inverter. However, the "area" under the pulse remains essentially the same.

It can be noted that in addition to the voltage spikes, the instantaneous value of the terminal voltage changes slightly at each commutation. This effect can be attributed to two causes corresponding to the two resistive terms in (59) and (60). First, since the line current changes suddenly, the stator IR drop changes as well, resulting in a change in terminal voltage. Secondly, since the rotor flux linkages must be maintained constant when currents are switched in the stator circuits, the mutual flux linkage is not constant but changes slightly so as to maintain constant rotor flux linkage. This change is reflected in the air-gap voltage, and hence, the terminal voltage. The magnitude of the effect depends upon the relative values of rotor resistance and rotor leakage and magnetizing reactances.

Fig. 6 shows a typical torque versus speed curve at 60 Hz excitation wherein the dc link current I_R has been adjusted such that the rated fundamental component of current flows in the motor lines. The torque plotted in Fig. 6 is the average value of pulsating torque shown in Fig. 5(b). It can be noted that the torque remains very small until the motor approaches synchronous speed, then rises rapidly. Also shown on Fig. 6 for purposes of comparison is the torque for a conventional voltage source. It can be noted that the peak torque for the controlled current case is considerably higher than the voltage case suggesting that operation from a current source may be superior to operation from a voltage source. Further investigation, however, reveals that this is not the case. The high peak torque is, rather, a result of how saturation has been incorporated into the analysis.

The magnetizing reactance which has been used for the calculation of Fig. 6 was a saturated value (x_m = 2.68 pu) obtained from a conventional no-load test at nominal voltage. This value was then maintained constant in the computer program. Although the assumption of a constant (saturated) magnetizing reactance is reasonable when the motor is excited from a voltage source, operation with a fixed amplitude current results in operation over a wide range of flux conditions. Hence, the magnetizing reactance changes widely and plays a more dominant role in motor behavior.

In order to demonstrate this effect, the magnitude of the air-gap voltage has also been plotted in Fig. 6. At low speeds the flux level in the motor is very low so that the motor is essentially unsaturated. As the motor approaches synchronous speed, the flux begins to rise rapidly. When the speed exceeds the value corresponding to the intersection of the current source and voltage source characteristics, the air-gap flux begins to rise beyond 1.0 pu indicating a very saturated condition. It is apparent that operating points near synchronous speeds yield results which are highly in error when the saturation effect is not properly accounted for.

In order to more accurately account for saturation, the slope ratio method of deMello and Walsh was adopted [18]. This method assumes that the nonfundamental air-gap flux components resulting from saturation do not contribute to torque production and do not result in appreciable harmonic voltages at the machine terminals. Hence, space harmonics can still be neglected and saturation can be introduced into the analysis by adjusting the magnetizing reactance x_m so that $x_m i_m$ equals the air-gap flux ψ_m on the air-gap saturation curve. The per unit air-gap flux is obtained by subtracting the stator leakage impedance drop from the no-load terminal voltage. This voltage is used to define a factor $K(\psi_m)$ such that

$$K(\psi_m) = x_m(\text{sat})/x_m(\text{unsat}) \tag{44}$$

where x_m(unsat) is the magnetizing reactance corresponding to the air-gap line and where

$$x_m(\text{sat}) = \psi_m/i_m. \tag{45}$$

In (45), ψ_m equals the fundamental component of air-gap voltage and, i_m equals the magnetizing current. That is

$$i_m = [(i_{qs}^s + i_{qr}'^s)^2 + (i_{ds}^s + i_{dr}'^s)^2]^{1/2}. \tag{46}$$

In terms of variables defined over the interval $0 \leq \omega_e t < \pi/3$

$$i_m = [[I_R(x_r' - x_m)/x_r' + i_Q]^2 + [-I_R(x_r - x_m')/\sqrt{3}x_r' - i_D]^2]^{1/2}. \tag{47}$$

Fig. 7 gives the slope ratio curve for the tested motor.

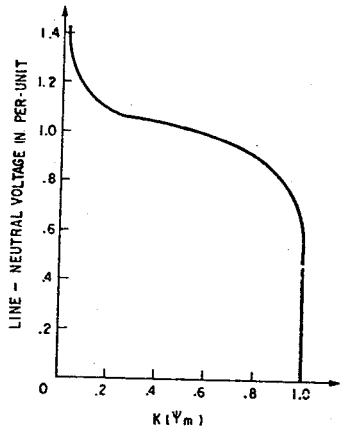

Fig. 7. Slope ratio curve.

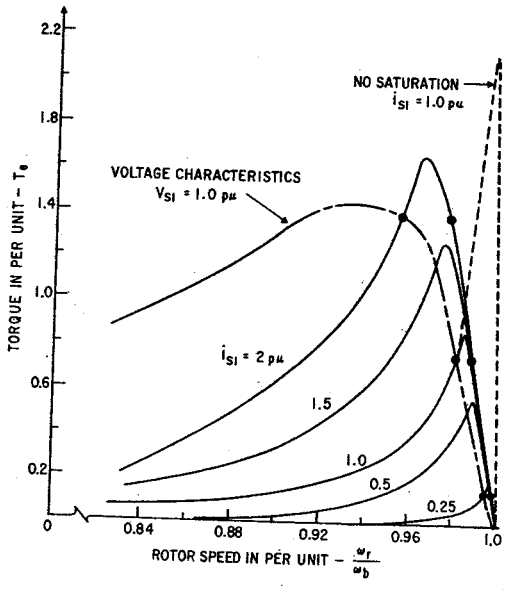

Fig. 8. Torque-speed curves for controlled current operation.

Although the solution with saturation is still represented in closed form, iteration must now be used to converge upon the proper value of $K(\psi_m)$ such that (45) is satisfied for the specified values of dc link current and motor speed. In Fig. 8 are shown a family of torque-speed curves wherein the effect of saturation has been included. The parameter i_{s1} is the fundamental component of motor line current rather than dc link current. In can be shown that i_{s1} is related to the dc link current by

$$i_{s1} = \frac{2\sqrt{3}}{\pi} I_R. \tag{48}$$

Also plotted for purposes of comparison is the characteristic for 1.0 pu current without saturation and for a conventional 1.0 pu voltage source. The large peak torque is clearly eliminated when saturation is accounted for.

MODES OF OPERATION

Examination of Fig. 9 suggests a number of possible modes of operation. a) The dc link current can simply be fixed at a value which ensures that breakdown torque

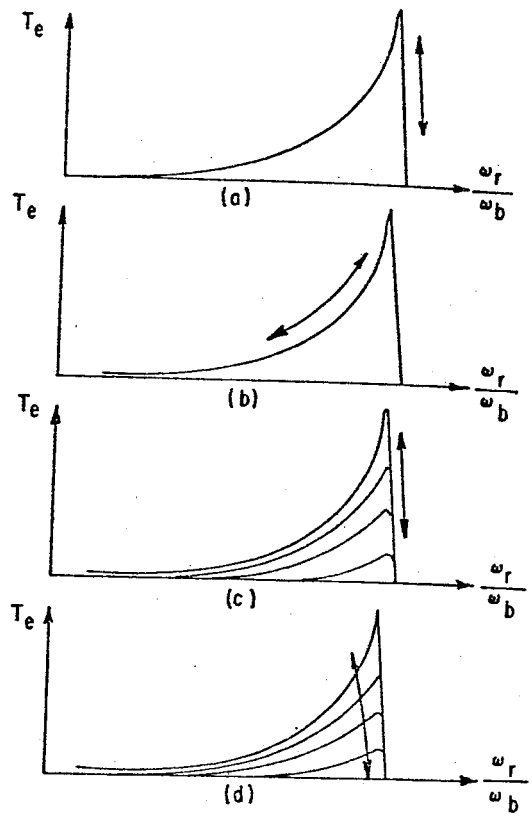

Fig. 9. Possible modes for controlled current operation.

is never exceeded. Operation is always on the stable negatively-sloped portion of the torque-speed characteristic. This mode would clearly result in a highly saturated condition and excessive heating in the motor, especially at light loads. b) The dc link current can be fixed at the same value as in a) and the motor operated on the positively-sloped portion of the curve. Although the motor is now unsaturated, motor heating is again high. Operation at light loads would be difficult. Since the positively-sloped portion of the curve is statically unstable, feedback would be necessary to ensure stable operation. c) The dc link current can be adjusted so that the motor always operates on the statically stable side of the curve at a speed slightly above the breakdown point. In this case stator heating would be less than in modes *a* and *b*, however, the motor would operate in a saturated condition. The dc link current and slip must be algebraically related so as to force this condition. d) The dc link current can be adjusted so that the motor operating points fall on the curve defined by the 1.0 pu voltage source. In this case performance would be closely analogous to operation from a voltage supply. Heating would again be minimal and the motor flux would be near its rated value. Link current and slip must again be related so as to force this condition. Since the motor operates on the statically unstable side of the motor torque-speed characteristic, a stabilization signal must be provided.

Since c) and d) appear to be the most desirable modes of operation, these two modes were compared at three typical operating conditions corresponding to light, rated,

TABLE I
PERFORMANCE CRITERIA (PER UNIT)

	Light Load i_{s1} = 0.25 pu		Rated Load i_{s1} = 1.0 pu		Heavy Load i_{s1} = 2.0 pu	
	Mode d	Mode c	Mode d	Mode c	Mode d	Mode c
Ave Torque	.13	.13	..76	..76	1.41	1.41
Pk-to-Pk Torque	.103	.132	.215	.566	.270	.888
Stator Loss	.0026	.0026	.042	.042	.167	.167
Rotor Loss	.0007	.0005	.017	.010	.070	.041

and heavy load. The six operating points selected are identified by the circles on Fig. 8. A summary of a number of performance criteria is given in Table I. It can be noted that the pulsating torque components are considerably higher for mode c) than for mode d). Since the stator current is the same in both cases the stator losses are, of course, the same. However, the rotor losses increase the case of mode d). The air-gap flux is considerably higher for mode c) suggesting also higher iron loss for this operating condition.

CONCLUSIONS

In this paper a detailed solution has been developed for the steady-state operation of an induction motor supplied from an ideal controlled current inverter source. Since the solution is obtained in closed form, iterative or superposition techniques, which approach the true solution only after numerous computational steps, are avoided entirely. The equations which have been derived are immediately applicable to transient solutions and can be extended, if necessary, to include the effects of finite source impedance. It was shown that saturation has an important effect on motor performance. The slope ratio method was incorporated to account for this effect. Investigation of feasible operating points indicates that if the motor is to remain unsaturated, feedback control is required in order to achieve stable operation.

APPENDIX I

The differential equations which define the voltages are given by the equations corresponding to the first two rows of (1)

$$v_{qs}^{s} = r_s i_{qs}^{s} + x_s \frac{p}{\omega_b} i_{qs}^{s} + x_m \frac{p}{\omega_b} i_{qr}'^{s} \tag{49}$$

$$v_{ds}^{s} = r_s i_{ds}^{s} + x_s \frac{p}{\omega_b} i_{ds}^{s} + x_m \frac{p}{\omega_b} i_{dr}'^{s}. \tag{50}$$

When the voltages are expressed in terms of the pseudocurrent variables, (49) and (50) become

$$v_{qs}^{s} = r_s i_{qs}^{s} + \frac{x_s x_r' - x_m^2}{x_r'} \frac{p}{\omega_b} i_{qs}^{s} + x_m \frac{p}{\omega_b} i_Q \tag{51}$$

$$v_{ds}^{s} = r_s i_{ds}^{s} + \frac{x_s x_r' - x_m^2}{x_r'} \frac{p}{\omega_b} i_{ds}^{s} + x_m \frac{p}{\omega_b} i_D. \tag{52}$$

Reference to Fig. 4 indicates that during state 1

$$i_{qs}^{s} = I_R \tag{53}$$

$$i_{ds}^{s} = \frac{I_R}{\sqrt{3}} - \frac{2I_R}{\sqrt{3}} u(t) \tag{54}$$

where $u(t)$ is the unit step function defined so that $u(t) = 0$ for $t < 0$, and $u(t) = 1$ for $t \geq 0$. Differentiating (53) and (54) it is apparent that over the specified interval

$$\frac{p}{\omega_b} i_{qs}^{s} = 0 \tag{55}$$

$$\frac{p}{\omega_b} i_{ds}^{s} = \frac{-2I_R}{\sqrt{3}\omega_b} \delta(t) \tag{56}$$

where $\delta(t)$ is the impulse function defined as the derivative of the unit step function.

Substituting these results into (46) and (47) yields

$$v_{qs}^{s} = r_s I_R + x_m \frac{p}{\omega_b} i_Q \tag{57}$$

$$v_{ds}^{s} = \frac{-r_s I_R}{\sqrt{3}} - \frac{x_s x_r' - x_m^2}{\omega_b x_r'} \frac{2I_R}{\sqrt{3}} \delta(t) + x_m \frac{p}{\omega_b} i_D. \tag{58}$$

The reactance factor $(x_s x_r' - x_m^2)/x_r'$ can be recognized as the stator transient reactance and is essentially equal to the sum of the stator plus rotor leakage reactance. The derivative terms $(p/\omega_b) i_Q$ and $(p/\omega_b) i_D$ are known from (19). Eliminating these terms from (57) and (58) yields the $d - q$ stator voltages uniquely in terms of the dc link current and $d - q$ pseudocurrents.

$$v_{qs}^{s} = \left[r_s + r_r' \frac{x_m^2}{(x_r')^2} \right] I_R - r_r' \frac{x_m}{x_r'} i_Q + \frac{\omega_r}{\omega_b} x_m i_D \tag{59}$$

$$v_{ds}^{s} = -\frac{1}{\sqrt{3}} \left[r_s + r_r' \frac{x_m^2}{(x_r')^2} \right] I_R - \frac{x_s x_r' - x_m^2}{\omega_b x_r'} \frac{2I_R}{\sqrt{3}} \delta(t) - r_r' \frac{x_m}{x_r'} i_D - \frac{\omega_r}{\omega_b} x_m i_Q. \tag{60}$$

The phase voltages are readily found from the inverse equations to (2) and (3)

$$v_{as} = \left[r_s + r_r' \frac{x_m^2}{(x_r')^2} \right] I_R - r_r' \frac{x_m}{x_r'} i_Q + \frac{\omega_r}{\omega_b} x_m i_D \tag{61}$$

$$v_{bs} = \frac{r_r' x_m}{x_r'} \left(\frac{i_Q}{2} + \frac{\sqrt{3}}{2} i_D \right) + \frac{\omega_r}{\omega_b} x_m \left(\frac{\sqrt{3}}{2} i_Q - \frac{1}{2} i_D \right) + \frac{x_s x_r' - x_m^2}{\omega_b x_r'} I_R \delta(t) \tag{62}$$

$$v_{cs} = -\left[r_s + r_r' \frac{x_m^2}{(x_r')^2} \right] I_R + \frac{r_r' x_m}{x_r'} \left(\frac{i_Q}{2} - \frac{\sqrt{3}}{2} i_D \right) - \frac{\omega_r}{\omega_b} x_m \cdot \left(\frac{\sqrt{3}}{2} i_Q + \frac{1}{2} i_D \right) - \frac{x_s x_r' - x_m^2}{\omega_b x_r'} I_R \delta(t). \tag{63}$$

Substituting (13) and (14) into (8), the electromagnetic torque expressed in terms of the stator currents and modified rotor currents is

$$T_e = x_m(i_{qs}{}^s i_D - i_{ds}{}^s i_Q). \tag{64}$$

Over interval 1 wherein $0 \leq \omega_e t < \pi/3$, the stator currents are given by (37), Hence, the electromagnetic torque over this interval is given by

$$T_e = x_m I_R \left[i_D + \frac{1}{\sqrt{3}} i_Q \right]. \tag{65}$$

APPENDIX II

Nameplate Motor Data

18.65 kW
4-pole
3-phase Y-connected
$\omega_b = 377$ rad/s
$V_{\text{rated}} = 230$ V rms line-to-line
$I_{\text{rated}} = 64$ A rms

Base Quantities

$V_{\text{Base}} = 187.8$ V
$I_{\text{Base}} = 90.5$ A
$T_{\text{Base}} = 135.2$ N·m

Motor Parameters	SI Units	Per Unit
r_s	0.0788	0.0380
r_r'	0.0408	0.0197
x_s	5.75	2.77
x_r'	6.00	2.89
$x_{m(\text{sat})}$	5.54	2.68
$x_{m(\text{unsat})}$	9.33	4.50

REFERENCES

[1] A. H. Mittag, "Electric valve converting apparatus," U. S. Patent 1 946 292, Feb. 6, 1934.
[2] C. Adamson and N. G. Hingorani, *High Voltage Direct Current Power Transmission.* London: Garraway, 1960.
[3] M. Z. Khamudkhanov, *Frequency Control of Asynchronous Electric Drives with the Aid of Autonomous Inverters* (in Russian). Tashkent, Uzbek, SSR: Academy of Science, 1959.
[4] E. E. Ward, "Invertor suitable for operation over a range of frequency," *Proc Inst. Elec. Eng.*, vol. 111, pp. 1423–1434, Aug. 1964.
[5] F. Blaschke, H. Ripperger, and H. Steinkonig, "The control of induction motors with thyristor frequency converters for impressed stator current" (in German), *Siemens-Z.*, vol. 42, (9), pp. 773–777, 1968.
[6] M. Z. Khamudkhanov and A. A. Khashimov, *Theory and Methods of Calculation for Frequency Controlled Asynchronous Electric Drives for Asymmetrical Conditions* (in Russian). Tashkent, Uzbek, SSR: FAN, 1969.
[7] S. G. Zabrovski, G. B. Lazarev, A. V. Natalkin, and U. G. Tolstov, "The static characteristics of a frequency control system for an induction motor using current inversion" (in Russian), *Elektrichestvo*, pp. 38–41, Aug. 1971.
[8] P. G. Sperling, "The static converter fed induction motor operated with impressed square-wave current," *Siemens-Z.*, vol. 45, pp. 508–514, Aug. 1971.
[9] K. P. Phillips, "Current source inverter for ac motor drives," *IEEE Trans. Ind. Appl.*, vol. IA-8, pp. 679–683, Nov./Dec. 1972.
[10] M. B. Brennan, "A comparative analysis of two commutation circuits for adjustable current input inverters feeding induction motors," in *Conf. Rec. 1973 IEEE Power Electron. Specialists Conf.*, pp. 201–212.
[11] W. Farrer and J. D. Miskin, "Quasi-sine wave fully regenerative invertor," *Proc. Inst. Elec. Eng.*, vol. 120, pp. 969–976, Sept. 1973.
[12] W. V. Lyon, *Transient Analysis of Alternating Current Machinery.* New York: Technology M.I.T. and Wiley, 1954.
[13] P. C. Krause, "Method of multiple reference frames applied to the analysis of symmetrical induction machinery," *IEEE Trans. Power App. Syst.*, vol. PAS-87, pp. 218–227, Jan. 1968.
[14] D. Novotny and A. F. Fath, "The analysis of induction machines controlled by series connected semiconductor switches," *IEEE Trans. Power App. Syst.*, vol. PAS-87, pp. 597–605, Feb. 1968.
[15] T. A. Lipo, "The analysis of induction motors with symmetrically triggered thyristors," *IEEE Trans. Power App. Syst.*, vol. PAS-90, pp. 515–525, Mar./Apr. 1971.
[16] H. C. Stanley, "An analysis of the induction machine," *AIEE Trans.*, vol. 57, pp. 751–757, 1938.
[17] P. C. Krause and C. H. Thomas, "Simulation of symmetrical induction machinery," *IEEE Trans. Power App. Syst.*, vol. PAS 84, pp. 1038–1053, Nov. 1965.
[18] F. P. deMello and G. W. Walsh, "Reclosing transients in induction motors with terminal capacitors," *AIEE Trans. Power App. Syst.*, vol. 80, pp. 1206–1213, Feb. 1961.

Thomas A. Lipo (M'64–SM'72) was born in Milwaukee, Wis., on February 1, 1938. He received the B.E.E. degree with honors and the M.S.E.E. degree from Marquette University, Milwaukee, in 1962 and 1964, respectively, and the Ph.D. degree in electrical engineering from the University of Wisconsin, Madison, in 1968.

From 1959 to 1964, he completed both the Cooperative Training Course and the Graduate Training Course at the Allis-Chalmers Manufacturing Company, Milwaukee, Wis. During 1968–1969, he was a S.R.C. Postdoctoral Fellow at the University of Manchester Institute of Science and Technology, Manchester, England. Since 1969, he has been an Electrical Engineer in the Physics and Electrical Engineering Laboratory, Research and Development Center, of the General Electric Company, Schenectady, N.Y. During the academic year 1973–1974, he was a visiting Associate Professor at Purdue University, West Lafayette, Ind. At General Electric, he has been engaged in the simulation, analysis, and control of static converter systems for a variety of applications including linear motors, static exciters, ball mills, turbine-generator rotor balancing, and traction drives for rail and off-highway vehicles.

Dr. Lipo is a member of Eta Kappa Nu, Pi Mu Epsilon, Tau Beta Pi, and Sigma Xi.

Edward P. Cornell (S'69–M'72) received the B.E.E. degree from Ohio State University, Columbus, in 1967, and the M.S.E.E. and Ph.D. degrees from the University of Wisconsin, Madison, in 1969 and 1972, respectively.

From 1967 to 1971 he was an Electrical Engineering Instructor at the University of Wisconsin. He taught courses in machine theory relating to synchronous and induction machine transient behavior. In 1972 he joined the research staff of the General Electric Company, Schenectady, N.Y., where he has been involved in the analysis and advanced development of adjustable speed drives and special purpose power systems. This work has included the development of digital simulation techniques for the prediction of transient performance of open- and closed-loop induction and synchronous motor drives, and the development of hybrid computer simulations of statically fed ac and dc drive systems. He has extensive laboratory experience in the testing and evaluation of solid-state powered drives. He is currently involved in the design of special purpose motors and the analysis and prediction of motor performance when operating from solid-state power supplies.

Dr. Cornell is a member of Eta Kappa Nu and Sigma Xi.